




Article

Franksousaite, $\text{PbCu}(\text{Se}^{6+}\text{O}_4)(\text{OH})_2$, the Se^{6+} analogue of linarite, a new mineral from the El Dragón mine, Potosí, Bolivia

Hexiong Yang* , James A. McGlasson, Ronald B. Gibbs and Robert T. Downs

Department of Geosciences, University of Arizona, 1040 E. 4th Street, Tucson, AZ 85721-0077, USA

Abstract

A new mineral species, franksousaite (IMA2021-096), ideally $\text{PbCu}(\text{Se}^{6+}\text{O}_4)(\text{OH})_2$, has been found from the El Dragón mine, Antonio Quijarro Province, Potosí Department, Bolivia. It occurs as short prismatic crystals included in colourless anglesite. Associated minerals are Co-bearing kruit'aite–penroseite, chalcomenite, schmiederite, olsacherite, phosgenite, anglesite and cerussite. Franksousaite is blue in transmitted light, transparent with very pale blue streak and has a vitreous lustre. It is brittle and has a Mohs hardness of 2–2½. Cleavage is perfect on {100}. The calculated density is 5.64 g/cm³. An electron microprobe analysis yielded an empirical formula (based on 6 O apfu) of $\text{Pb}_{1.02}\text{Cu}_{0.98}[(\text{Se}_{0.84}\text{S}_{0.17})_{\Sigma 1.01}\text{O}_4](\text{OH})_2$, which is simplified to $\text{PbCu}[(\text{Se,S})\text{O}_4](\text{OH})_2$.

Franksousaite is the Se^{6+} analogue of linarite, $\text{PbCu}(\text{SO}_4)(\text{OH})_2$. It is monoclinic, with space group $P2_1/m$ and unit-cell parameters $a = 9.8208(3)$, $b = 5.7340(2)$, $c = 4.74980(10)$ Å, $\beta = 102.683(2)^\circ$, $V = 260.947(13)$ Å³ and $Z = 2$. The crystal structure of franksousaite consists of Jahn-Teller-distorted Cu^{2+}O_6 square bipyramids, which form chains along b by sharing *trans* edges across their square planes. The chains are decorated by SeO_4 tetrahedra and linked to one another by hydrogen bonds to form layers parallel to (100). These layers are bound together by double layers of PbO_8 and SeO_4 polyhedra. The PbO_8 polyhedron exhibits one-sided coordination typical of Pb^{2+} with a stereochemically active 6s² lone-electron-pair. The major structural difference between franksousaite and linarite lies in the $\langle \text{Se}-\text{O} \rangle$ vs. $\langle \text{S}-\text{O} \rangle$ bond distances (1.615 vs. 1.482 Å), accounting for the larger unit-cell volume for franksousaite. A comparison of Raman spectra for the four minerals in the linarite group (linarite, franksousaite, munakataite and schmiederite) reveals the obvious differences among them, especially in the range from 700 to 1000 cm⁻¹, indicative of the presence or absence of $(\text{Se}^{4+}\text{O}_3)^{2-}$, $(\text{Se}^{6+}\text{O}_4)^{2-}$, and/or $(\text{SO}_4)^{2-}$ groups.

Keywords: franksousaite, linarite, new mineral, crystal structure, Raman, El Dragón mine, Bolivia

(Received 8 June 2022; accepted 21 July 2022; Accepted Manuscript published online: 27 July 2022; Associate Editor: Elena Zhitova)

Introduction

Franksousaite, ideally $\text{PbCu}(\text{Se}^{6+}\text{O}_4)(\text{OH})_2$, is a new mineral species from the El Dragón mine, Antonio Quijarro Province, Potosí Department, Bolivia. It is named in honour of Mr. Francis (Frank) X. Sousa (born in 1951). Frank's interest in minerals began at age 9 and he started collecting minerals, especially Pb-bearing minerals, in his teenage years. He received his B.S. degree in geology from Oklahoma State University in 1973 and M.S. degree in mineralogy, petrology and economic geology from the University of Arizona in 1980. Since joining the Tucson Gem and Mineral Society in 1976, Frank has served as recording secretary, property manager, collection manager, show floor setup manager and guest exhibit chair. In particular, he has been actively involved in youth education activities related to mineral collecting and identifications. Frank is a highly dedicated volunteer and takes great pride in it with his outstanding knowledge and experience in mineralogy. Since 2016, he has

been a volunteer at the Arizona Sonora Desert Museum, the University of Arizona Mineral Museum and the University of Arizona Mineralogy Laboratory at the Department of Geosciences. In addition, Frank voluntarily taught several classes on geology and mineralogy to senior citizens through the University of Arizona's Osher Lifelong Learning Institute and on mineral identifications at Pima Community College in Tucson, Arizona. He has helped Boy Scouts earn the Geology Merit Badge and performed advisory judging for 4H youth rock-collection displays. One of Frank's great joys for mineral collecting is to gift specimens to both youths and adults and to share interesting geological stories behind them. The new mineral and its name have been approved by the Commission on New Minerals, Nomenclature and Classification (CNMNC) of the International Mineralogical Association (IMA2021-096, Yang *et al.*, 2022). The co-type samples have been deposited at the University of Arizona Alfie Norville Gem and Mineral Museum (Catalogue # 22713) and the RRUFF Project (deposition # R210012) (<http://rruff.info>) (Lafuente *et al.*, 2015). This paper describes the physical and chemical properties of franksousaite, and its crystal structure determined from single-crystal X-ray diffraction data, illustrating its structural relationships to the minerals of the linarite group.

*Author for correspondence: Hexiong Yang, Email: hyang@arizona.edu

Cite this article: Yang H., McGlasson J.A., Gibbs R.B. and Downs R.T. (2022) Franksousaite, $\text{PbCu}(\text{Se}^{6+}\text{O}_4)(\text{OH})_2$, the Se^{6+} analogue of linarite, a new mineral from the El Dragón mine, Potosí, Bolivia. *Mineralogical Magazine* 86, 792–798. <https://doi.org/10.1180/mgm.2022.90>

© The Author(s), 2022. Published by Cambridge University Press on behalf of The Mineralogical Society of Great Britain and Ireland. This is an Open Access article, distributed under the terms of the Creative Commons Attribution licence (<http://creativecommons.org/licenses/by/4.0/>), which permits unrestricted re-use, distribution and reproduction, provided the original article is properly cited.



Fig. 1. The specimen on which the new mineral franksousaite, indicated by the blue arrow, was found.

Sample description and experimental methods

Occurrence, physical and chemical properties, and Raman spectra

Franksousaite was found on a specimen (Fig. 1) collected from the El Dragón mine (19°49'15''S, 65°55'0''W), Antonio Quijarro Province, Potosí Department, Bolivia. Associated minerals are Co-bearing krut'aite-penroseite, chalcomenite, schmiederite, olsacherite, phosgenite, anglesite, and cerussite. Detailed descriptions on the geology and mineralogy of the El Dragón mine have been given by Grundmann *et al.* (1990, 2007) and Grundmann and Förster (2017). This mine exploited a telethermal deposit consisting of a single selenide vein hosted in sandstones and shales. The major ore mineral is krut'aite, CuSe_2 , varying in composition to penroseite, NiSe_2 . Subsequent solutions rich in Bi, Pb and Hg resulted in the crystallisation of minerals such as clausenthalite, petrovicite, watkinsonite, and the recently described minerals eldragónite, $\text{Cu}_6\text{BiSe}_4(\text{Se}_2)$ (Paar *et al.*, 2012), grundmannite, CuBiSe_2 (Förster *et al.*, 2016), hansblockite, $(\text{Cu,Hg})(\text{Bi,Pb})\text{Se}_2$ (Förster *et al.*, 2017), cerromojonite, CuPbBiSe_3 (Förster *et al.*, 2018) and nickeltyrrellite, CuNi_2Se_4 (Förster *et al.*, 2019). Oxidation produced a wide range of secondary Se-bearing minerals, such as favreauite, $\text{PbBiCu}_6\text{O}_4(\text{SeO}_3)_4(\text{OH})\cdot\text{H}_2\text{O}$ (Mills *et al.*, 2014), alfredopetrovite, $\text{Al}_2(\text{Se}^{4+}\text{O}_3)_3\cdot 6\text{H}_2\text{O}$ (Kampf *et al.*, 2016a) and the new mineral franksousaite, described herein.

Franksousaite occurs as blue prismatic crystals included in colourless anglesite (Figs 2 and 3), which is on a matrix consisting of Co-bearing krut'aite-penroseite. Individual crystals of franksousaite are found up to $0.05 \times 0.02 \times 0.02$ mm. The blueish anglesite crystal in Fig. 2 was picked out and broken into small pieces (Fig. 3) in order to extract franksousaite crystals for the necessary analyses and measurements. In total, four tiny franksousaite crystals were recovered, but they all have some anglesite attached to them. It is very difficult, if not entirely impossible, to completely separate anglesite from franksousaite while trying to maintain the largest crystal sizes for the analyses and measurements. In Fig. 3, crystal A was used for the electron microprobe analysis and crystal B for X-ray diffraction data collection and then Raman spectral measurement. The blue portion on the left side of crystal B in Fig. 3 is a single crystal of franksousaite and the colourless portion on the right side a single crystal of anglesite. Although the collected X-ray diffraction data were from both franksousaite and

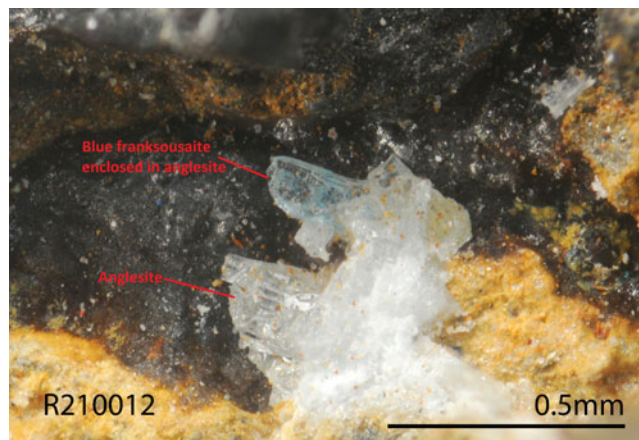


Fig. 2. A microscopic view of blue franksousaite enclosed in a large colourless anglesite crystal, making the whole anglesite crystal look blueish.

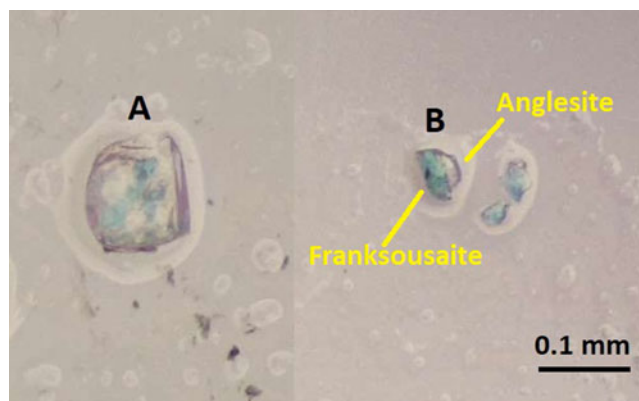


Fig. 3. Broken fragments of blue franksousaite crystals enclosed in the large colourless anglesite crystal in Fig. 2. Crystal A was used for the electron microprobe analysis. Crystal B was used for X-ray diffraction data collection and then Raman spectral measurement.

Table 1. Analytical chemical compositions (in wt.%) for franksousaite.

Constituent	Mean	Range	S.D.	Probe standard
PbO	51.17	50.87–51.54	0.26	wulfenite
CuO	17.42	17.04–17.77	0.22	chalcocopyrite
SeO ₃	23.82	23.53–24.04	0.24	ZnSe (synthetic)
SO ₃	2.98	2.55–3.21	0.29	baryte
H ₂ O	4.04			
Total*	99.43	98.77–100.03	0.32	

*Trace amounts of Si, Cr and Te were detected by energy dispersive spectroscopy, however they were below the measurement limits ($<3\sigma$) by WDS. The H₂O content was added to achieve the ideal value of 2H apfu.

anglesite crystals, they can be separated easily for the structure analysis (see the Structure section below for more details). The black spot on the left side of crystal B in Fig. 3 was caused by burning during the Raman data collection with the 532-nm laser at the full power of 150 mW. Therefore, the Raman data were collected at the 50% power of 150 mW (see the Raman section below).

Franksousaite is blue in transmitted light, transparent with very pale blue streak and vitreous lustre. It is brittle and has a

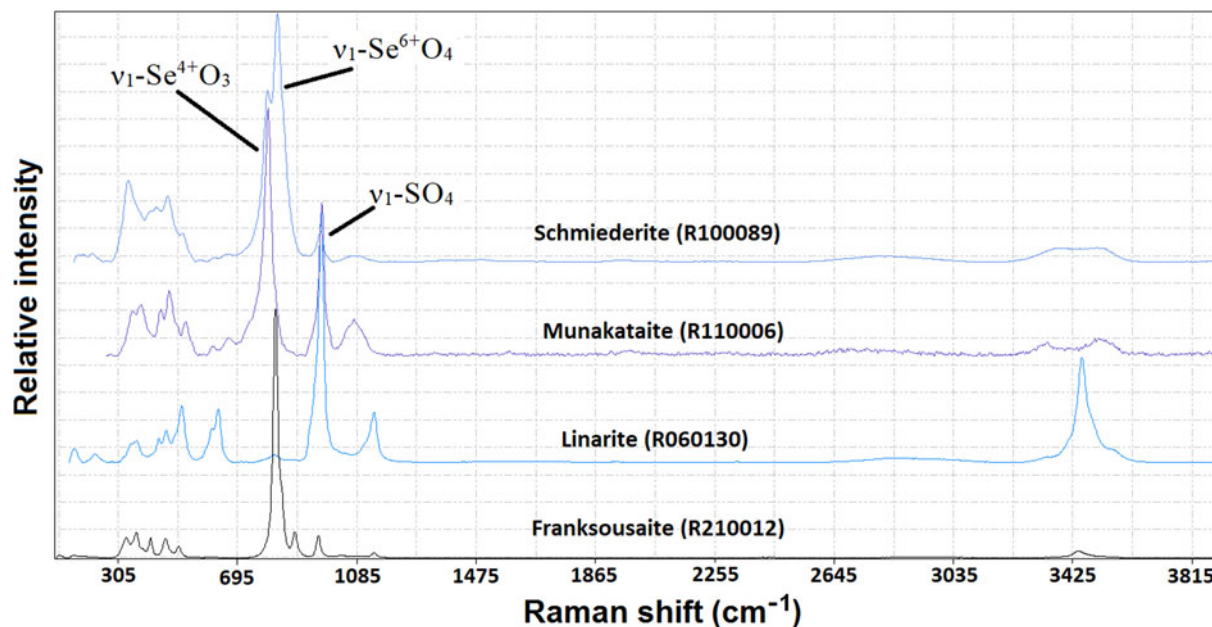


Fig. 4. Raman spectra of franksousaite, linarite, munakataite and schmiederite.

Mohs hardness of 2–2½. Cleavage could not be determined due to the small crystal size. By its structural analogue to linarite, it should have perfect cleavage on {100}. The density could not be measured due to the small crystals and intergrowth with anglesite. The calculated density is 5.64 g/cm³ on the basis of the empirical chemical formula and unit cell volume from single-crystal X-ray

diffraction data. No optical data were measured due to the intergrowth with anglesite. The Gladstone–Dale relationship (Mandarino, 1981) gives $n = 1.88$. Franksousaite is insoluble in water and hydrochloric acid.

The chemical composition was determined using a Cameca SX-100 electron microprobe (wavelength dispersive spectroscopy mode, 15 kV, 10 nA and a beam diameter of 2 μm). The standards used for the probe analysis are given in Table 1, along with the determined compositions (5 analysis points). The resultant chemical formula, calculated on the basis of 6 O atoms per formula unit (apfu) (from the structure determination), is

Table 2. Powder X-ray diffraction data for franksousaite.

l_{obs}	l_{calc}	d_{obs}	d_{calc}	h	k	l
22	30	9.548	9.580	1	0	0
24	38	4.917	4.917	1	1	0
35	64	4.578	4.588	1	0	1
8	15	3.672	3.675	2	1	0
60	100	3.602	3.603	0	1	1
100	94	3.193	3.193	3	0	0
	(83)		(3.198)	(1	1	1)
50	92	3.150	3.151	2	1	1
8	16	3.014	3.014	2	0	1
15	32	2.856	2.865	0	2	0
20	39	2.746	2.744	1	2	0
21	41	2.621	2.624	3	1	1
5	17	2.436	2.437	0	2	1
10	24	2.347	2.350	4	0	1
15	21	2.296	2.294	2	0	2
14	17	2.209	2.194	1	1	2
18	21	2.145	2.146	1	0	2
4	6	2.055	2.056	3	2	1
9	19	1.853	1.853	4	1	1
21	18	1.828	1.828	1	2	2
7	8	1.791	1.791	2	2	2
5	11	1.765	1.766	0	3	1
10	13	1.705	1.704	2	3	1
14	9	1.597	1.597	6	0	0
5	10	1.576	1.576	4	2	2
5	8	1.522	1.524	1	1	3
4	9	1.431	1.432	0	4	0
5	9	1.308	1.307	3	4	0
7	5	1.215	1.215	2	4	2

The strongest lines are given in bold.

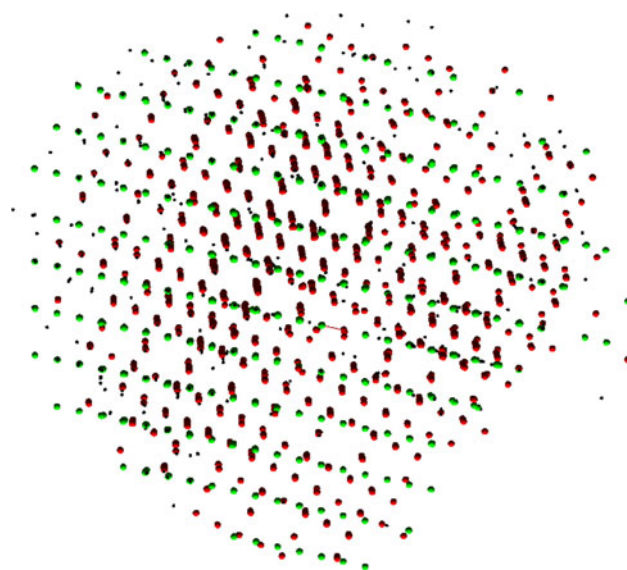


Fig. 5. A reciprocal space view of X-ray diffraction data collected from crystal B in Fig. 3. The green and red spots are for franksousaite and anglesite, respectively. Small black spots represent weak reflections [$I < 3\sigma(I)$]. The view is along the b axis of franksousaite. There are no obvious overlaps between the two lattice points.

Table 3. Comparison of crystallographic data and refinement results for minerals in the linarite group.

	Franksousaite	Linarite	Munakataite	Schmiederite
Ideal chemical formula	PbCu(SeO ₄)(OH) ₂	PbCu(SO ₄)(OH) ₂	Pb ₂ Cu ₂ (Se ⁴⁺ O ₃)(SO ₄)(OH) ₄	Pb ₂ Cu ₂ (Se ⁴⁺ O ₃)(Se ⁶⁺ O ₄)(OH) ₄
Crystal symmetry	Monoclinic	Monoclinic	Monoclinic	Monoclinic
Space group	<i>P</i> 2 ₁ / <i>m</i>	<i>P</i> 2 ₁ / <i>m</i>	<i>P</i> 2 ₁ / <i>m</i>	<i>P</i> 2 ₁ / <i>m</i>
<i>a</i> (Å)	9.8208(3)	9.701(2)	9.8023(26)	9.922(3)
<i>b</i> (Å)	5.7340(2)	5.650(2)	5.6751(14)	5.712(2)
<i>c</i> (Å)	4.74980(10)	4.690(2)	9.2811(25)	9.396(3)
β (°)	102.683(2)	102.65(2)	102.443(6)	101.96(3)
<i>V</i> (Å ³)	260.947(13)	250.82	504.2(2)	520.95
<i>Z</i>	2	2	4	2
ρ _{cal} (g/cm ³)	5.59	5.31	5.31	5.63
2θ range for data collection	≤66.34	≤90	≤41.58	≤55
No. of reflections collected	4117	4506	8377	2427
No. of independent reflections	1090	2207	590	1308
No. of reflections with <i>I</i> > 2σ(<i>I</i>)	1016	1991	544	1131
No. of parameters refined	56	53	106	63
R(int)	0.027			
Final <i>R</i> ₁ , <i>wR</i> ₂ factors [<i>I</i> > 2σ(<i>I</i>)]	0.020, 0.040	0.038, 0.034	0.031, 0.063	0.058, 0.055
Goodness-of-fit	1.113			1.093
Reference	This study	Effenberger (1987)	Kampf <i>et al.</i> (2010)	Effenberger (1987)

Pb_{1.02}Cu_{0.98}[(Se_{0.84}S_{0.17})Σ_{1.01}O₄](OH)₂, which can be simplified to PbCu[(Se,S)O₄](OH)₂.

The Raman spectrum of franksousaite (Fig. 4) was collected on a randomly oriented crystal with a Thermo Almega microRaman system, using a solid-state laser with a wavelength of 532 nm at 50% of 150 mW power and a thermoelectric cooled CCD detector. The laser is partially polarised with 4 cm⁻¹ resolution and a spot size of 1 μm.

X-ray crystallography

Both the powder and single-crystal X-ray diffraction data for franksousaite were collected on a Bruker APEX2 CCD X-ray diffractometer equipped with graphite-monochromatised MoKα radiation. Listed in Table 2 are the measured powder X-ray diffraction data. The unit-cell parameters obtained from the powder X-ray diffraction data using the program by Downs *et al.* (1993) are: *a* = 9.823(7), *b* = 5.729(2), *c* = 4.751(3) Å, β = 102.78(8)° and *V* = 260.8(2) Å³.

Single-crystal X-ray diffraction data were collected from a fragment containing both franksousaite and anglesite single crystals (crystal B in Fig. 3) with frame widths of 0.5° in ω and 30 s counting time per frame. Using the Bruker software CELL_NOW (Sevvana *et al.*, 2019), the X-ray diffraction data of franksousaite

Table 4. Fractional atomic coordinates and equivalent isotropic displacement parameters (Å²) for franksousaite.

Atom	<i>x/a</i>	<i>y/b</i>	<i>z/c</i>	<i>U</i> _{iso} [*] / <i>U</i> _{eq}
Pb	0.33388(2)	¼	0.33445(4)	0.01828(7)
Cu	0	0	0	0.00905(11)
Se ^{**}	0.33381(5)	¾	0.88515(10)	0.00846(15)
S ^{**}	0.33381(5)	¾	0.88515(10)	0.00846(15)
O1	0.4894(4)	¾	0.0750(8)	0.0187(7)
O2	0.3345(4)	¾	0.5464(7)	0.0265(9)
O3	0.2467(2)	0.5206(4)	0.9443(5)	0.0172(5)
O4	0.0343(3)	¾	0.2786(6)	0.0108(6)
H1	0.117(3)	¾	0.371(11)	0.016*
O5	0.0898(3)	¼	0.2692(6)	0.0096(6)
H2	0.072(6)	¼	0.434(6)	0.014*

** Occupancies < 1 : Se = 0.820(4) and S = 0.180(4)

and anglesite can be easily separated because the two crystals have different orientations and unit-cell dimensions (Fig. 5). The resultant intensity data for the two minerals are remarkably good and there are no obvious overlaps in the X-ray intensity data between the two minerals, as indicated by the subsequent structure refinements (*R*₁ = 0.020, *wR*₂ = 0.040, goodness-of-fit = 1.084 for franksousaite and *R*₁ = 0.0190, *wR*₂ = 0.031, goodness-of-fit = 1.072 for anglesite). All intensity data were corrected for X-ray absorption using the Bruker program SADABS (Bruker, 2001). The systematic absences of reflections suggest the possible space group *P*2₁ or *P*2₁/*m* for franksousaite and its structure was solved and refined using SHELX2018 (Sheldrick 2015a, 2015b) based on space group *P*2₁/*m*, because it produced better refinement statistics in terms of bond lengths and angles, atomic displacement parameters and *R* factors. All H atoms were located through the difference-Fourier syntheses. The structure refinement reveals that the Pb and Cu sites are fully filled by Pb and Cu, respectively, but the Se site has 18% Se substituted by S, consistent with the chemical composition determined from the electron microprobe analysis. All non-H atoms were refined anisotropically, whereas the two H atoms (H1 and H2) were refined isotropically. Final refinement statistics for franksousaite are listed in Table 3. Atomic coordinates and displacement parameters are given in Tables 4 and 5, respectively. Selected bond distances are presented in Table 6. The bond-valence sums were calculated using the parameters from Brown (2006) (Table 7). The crystallographic information file has been deposited with the Principal Editor of *Mineralogical Magazine* and is available as Supplementary material (see below).

Crystal structure description and discussion

Franksousaite is the Se⁶⁺ analogue of linarite, PbCu(SO₄)(OH)₂ (Bachmann and Zemmann, 1961; Araki, 1962; Effenberger, 1987; Schofield *et al.*, 2009). Its structure consists of Jahn-Teller-distorted Cu²⁺O₆ square bipyramids, which form chains along *b* by sharing *trans* edges across their square planes (Fig. 6). The chains are decorated by SeO₄ tetrahedra, which bond to apical corners of adjacent bipyramids. The chains are linked to one another by hydrogen bonds to form layers parallel to

Table 5. Atomic displacement parameters (\AA^2) for franksousaite.

	U^{11}	U^{22}	U^{33}	U^{12}	U^{13}	U^{23}
Pb	0.01218(10)	0.02074(11)	0.01890(11)	0	-0.00317(6)	0
Cu	0.0116(2)	0.0067(2)	0.0083(2)	-0.00077(18)	0.00101(18)	0.00016(16)
Se	0.0073(2)	0.0100(2)	0.0083(2)	0	0.00217(15)	0
S	0.0073(2)	0.0100(2)	0.0083(2)	0	0.00217(15)	0
O1	0.0126(16)	0.0183(18)	0.0240(18)	0	0.0018(13)	0
O2	0.023(2)	0.045(3)	0.0127(17)	0	0.0053(14)	0
O3	0.0119(11)	0.0122(12)	0.0257(12)	-0.0020(9)	0.0002(9)	0.0025(9)
O4	0.0108(14)	0.0108(16)	0.0101(14)	0	0.0010(11)	0
O5	0.0126(14)	0.0072(14)	0.0087(13)	0	0.0014(11)	0

(100), which are bound together by double layers of PbO_8 and SeO_4 polyhedra. The PbO_8 polyhedron exhibits one-sided coordination typical of Pb^{2+} with a stereochemically active $6s^2$ lone-electron-pair (Fig. 7). The major structural difference between franksousaite and linarite lies in the $\langle \text{Se-O} \rangle$ vs. $\langle \text{S-O} \rangle$ bond distances (Table 6), as the ionic radius of IVSe^{6+} (0.28 \AA) is significantly larger than that of S^{6+} (0.12 \AA) (Shannon 1976), accounting for the larger unit-cell volume for franksousaite.

In addition to franksousaite and linarite, the linarite group also includes munakataite $\text{Pb}_2\text{Cu}_2(\text{Se}^{4+}\text{O}_3)(\text{SO}_4)(\text{OH})_4$ and schmiederite $\text{Pb}_2\text{Cu}_2(\text{Se}^{4+}\text{O}_3)(\text{Se}^{6+}\text{O}_4)(\text{OH})_4$ (Table 3). Nevertheless, linarite and franksousaite are not isotypic, but show homeotypic relations with munakataite (Kampf *et al.*, 2010) or schmiederite (Effenberger, 1987), which have the c dimension doubled compared to linarite and franksousaite (Table 3), as a consequence of the ordering of Se^{4+}O_3 vs. SO_4 in munakataite or Se^{4+}O_3 vs. Se^{6+}O_4 in schmiederite.

Table 6. Selected bond distances (\AA) and angles ($^\circ$) for franksousaite and linarite.

	Franksousaite (This study)	Linarite (Schofield <i>et al.</i> , 2009)
Pb—O5	2.348(3)	2.351(4)
Pb—O3 $\times 2$	2.425(2)	2.421(3)
Pb—O1	2.877(3)	2.893(5)
Pb—O1	2.957(3)	2.933(4)
Pb—O2 $\times 2$	3.0381(12)	3.046(2)
Pb—O2	3.181(4)	3.048(6)
$\langle \text{Pb—O} \rangle$	2.786	2.770
Cu—O4 $\times 2$	1.929(2)	1.915(2)
Cu—O5 $\times 2$	1.993(2)	1.961(2)
Cu—O3 $\times 2$	2.497(2)	2.567(2)
$\langle \text{Cu—O} \rangle$	2.139	2.148
T—O1	1.594(3)	1.431(7)
T—O2	1.611(3)	1.496(8)
T—O3 $\times 2$	1.627(2)	1.485(5)
$\langle \text{T—O} \rangle$	1.615	1.474
O4—H1	0.83(2)	0.952(7)
H1...O2	2.12(2)	1.973(9)
O4...O2	2.943(5)	2.924(5)
$\angle \text{O4—H1...O2}$	172(5)	176.1(6)
O5—H2	0.84(2)	1.025(8)
H2...O4	1.89(2)	1.687(8)
O5...O4	2.692(4)	2.706(5)
$\angle \text{O5—H2...O4}$	159(5)	171.8(6)

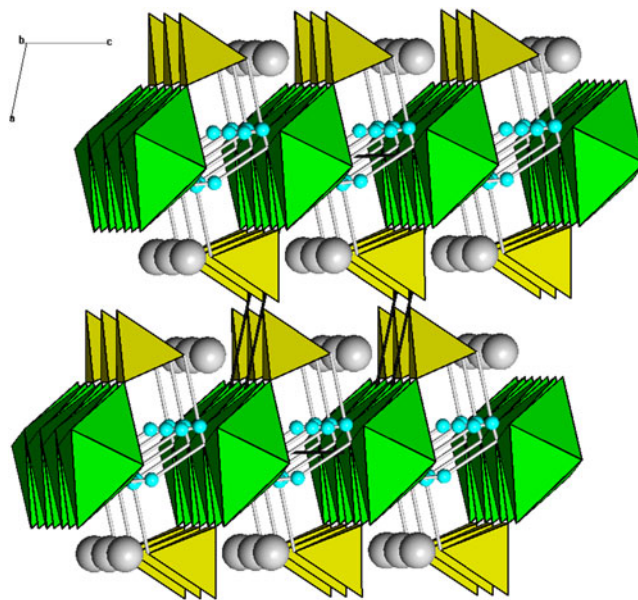
Note: T = Se for franksousaite and S for linarite.

Table 7. Bond-valence sums for franksousaite.

	Pb	Cu	Se*	Sum
O1	0.13		1.59	1.82
	0.10			
O2	0.08 $\times 2 \downarrow \rightarrow$		1.52	1.74
	0.06			
O3	0.43 $\times 2 \downarrow$	0.09 $\times 2 \downarrow$	1.46 $\times 2 \downarrow$	1.98
O4		0.42 $\times 2 \downarrow \rightarrow$		0.84
O5	0.53	0.36 $\times 2 \downarrow \rightarrow$		1.24
Sum	1.84	1.74	6.02	

*The bond valence sum for Se was calculated based on $(0.82\text{Se}^{6+} + 0.18\text{S}^{6+})$.

According to Raman spectroscopic studies on linarite (Buzgar *et al.*, 2009) and schmiederite (Frost and Keeffe, 2008), as well as other hydrous materials containing $(\text{Se}^{4+}\text{O}_3)^{2-}$, $(\text{Se}^{6+}\text{O}_4)^{2-}$, and/or $(\text{SO}_4)^{2-}$ (e.g. Wickleder *et al.*, 2004; Frost *et al.*, 2006; Djemel *et al.*, 2013; Wolak *et al.*, 2013; Kasatkin *et al.*, 2014; Mills *et al.*, 2014; Kampf *et al.*, 2016b), we made the following tentative assignments of major Raman bands for franksousaite. The weak peak at 3444 cm^{-1} is due to the O–H stretching vibrations in the OH groups. The small sharp bands at 932 and 1141 cm^{-1} ,

**Fig. 6.** Crystal structure of franksousaite. Green elongated octahedra and yellow tetrahedra represent CuO_6 and SeO_4 groups, respectively. Large grey and small aqua spheres represent Pb and H atoms, respectively. Hydrogen bonds are indicated by grey lines.

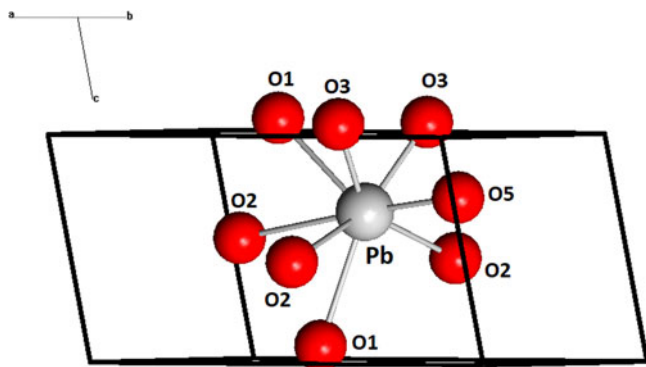


Fig. 7. The coordination of a Pb atom by eight O atoms in franksousaite.

resulting from the presence of a small amount of $(\text{SO}_4)^{2-}$ substituting for $(\text{SeO}_4)^{2-}$, can be attributed to the S–O symmetric and antisymmetric stretching vibrations within the SO_4 group, respectively. The strongest sharp band at 820 cm^{-1} and the weak band 882 cm^{-1} are ascribable to the Se–O symmetric and antisymmetric stretching modes, respectively, within the SeO_4 groups, whereas those from 300 to 530 cm^{-1} originate from the O–Se–O (and O–S–O) bending vibrations within the SeO_4 groups. The very weak bands below 300 cm^{-1} are associated mainly with the rotational and translational modes of SeO_4/SO_4 groups, as well as the Cu–O interactions and lattice vibrational modes.

The bond-valence sums indicate that O2 is noticeably underbonded (1.74 valence units). This deficiency is compensated by the hydrogen bond, as it is engaged in the hydrogen bonding as an acceptor (Table 7). According to the correlation between $\nu_{\text{O-H}}$ and O–H...O distances for minerals (Libowitzky, 1999), the Raman band at 3444 cm^{-1} corresponds well with the O–O distances between 2.70 and 2.95 \AA (O4–H1...O2 and O5–H2...O4).

For comparison, the Raman spectra of linarite (<http://rruff.info/R060130>), munakataite (<http://rruff.info/R110006>) and schmiederite (<http://rruff.info/R100089>), which are in the same mineral group as franksousaite, from the RRUFF Project are also plotted in Fig. 4. The spectral differences among the four minerals are obvious, especially in the range from 700 to 1000 cm^{-1} , indicative of the presence or absence of $(\text{SeO}_3)^{2-}$, $(\text{Se}^{6+}\text{O}_4)^{2-}$ and/or $(\text{SO}_4)^{2-}$ groups.

Acknowledgements. We are grateful for the constructive comments by Dr. Elena Zhitova and three other anonymous reviewers. This study was funded by the Feinglos family and Mr. Michael M. Scott.

Supplementary material. To view supplementary material for this article, please visit <https://doi.org/10.1180/mgm.2022.90>

Competing interests. The authors declare none.

References

- Araki T. (1962) The crystal structure of linarite, re-examined. *Mineralogical Journal*, **3**, 282–295.
- Bachmann H.G. and Zemann J. (1961) Die Kristallstruktur von Linarit, $\text{PbCuSO}_4(\text{OH})_2$. *Acta Crystallographica*, **14**, 747–753.
- Brown I.D. (2006) *Accumulated Table of Bond Valence Parameters*. http://www.ccp14.ac.uk/ccp/web-mirrors/i_d_brown/.
- Bruker (2001) *SADABS*. Bruker AXS Inc., Madison, Wisconsin, USA.
- Buzgar N., Buzatu A. and Sanislav I.V. (2009) The Raman study on certain sulfates. *Annalele Stiintifice ale Universitatii*, **55**, 5–23.

- Djemel M., Abdelhedi M., Ktari L. and Dammak M. (2013) X-ray diffraction, Raman study and electrical properties of the new mixed compound $\text{Rb}_{1.7}\text{K}_{0.3}(\text{SO}_4)_{0.88}(\text{SeO}_4)_{0.12}\text{Te}(\text{OH})_6$. *Journal of Molecular Structure*, **1047**, 15–21.
- Downs R.T., Bartelmehs K.L., Gibbs G.V. and Boisen M.B., Jr (1993) Interactive software for calculating and displaying X-ray or neutron powder diffractometer patterns of crystalline materials. *American Mineralogist*, **78**, 1104–1107.
- Effenberg H. (1987) Crystal structure and chemical formula of schmiederite $\text{Pb}_2\text{Cu}_2(\text{OH})_4(\text{SeO}_3)(\text{SeO}_4)$, with a comparison to linarite, $\text{PbCu}(\text{OH})_2(\text{SO}_4)$. *Mineralogy and Petrology*, **36**, 3–12.
- Förster H.-J., Bindi L. and Stanley C.J. (2016) Grundmannite, CuBiSe_2 , the Se-analogue of emplectite, a new mineral from the El Dragón mine, Potosí, Bolivia. *European Journal of Mineralogy*, **28**, 467–477.
- Förster H.-J., Bindi L., Stanley C.J. and Grundmann G. (2017) Hansblockite, $(\text{Cu,Hg})(\text{Bi,Pb})\text{Se}_2$, the monoclinic polymorph of grundmannite: a new mineral from the Se mineralization at El Dragón (Bolivia). *Mineralogical Magazine*, **81**, 229–240.
- Förster H.-J., Bindi L., Grundmann G. and Stanley C.J. (2018) Cerrromojonite, CuPbBiSe_3 , from El Dragón (Bolivia): A new member of the bournonite group. *Minerals*, **8**, 420.
- Förster H.-J., Ma C., Grundmann G., Bindi L. and Stanley C.J. (2019) Nickelytyrellite, CuNi_2Se_4 , a new member of the spinel supergroup from El Dragón, Bolivia. *The Canadian Mineralogist*, **57**, 637–646.
- Frost R.L. and Keefe E.C. (2008) Raman spectroscopic study of the schmiederite $\text{Pb}_2\text{Cu}_2[(\text{OH})_4(\text{SeO}_3)(\text{SeO}_4)]$. *Journal of Raman Spectroscopy*, **39**, 1408–1402.
- Frost R.L., Weier M.L., Reddy B.J. and Čejka J. (2006) A Raman spectroscopic study of the uranyl selenite mineral haynesite. *Journal of Raman Spectroscopy*, **37**, 816–821.
- Grundmann G. and Förster H.-J. (2017) Origin of the El Dragón selenium mineralization, Quijarro Province, Potosí, Bolivia. *Minerals*, **7**, 1–68.
- Grundmann G., Lehrberger G. and Schnorrer-Köhler G. (1990) The El Dragón mine, Potosí, Bolivia. *Mineralogical Record*, **21**, 133–150.
- Grundmann G., Lehrberger G. and Schnorrer-Köhler G. (2007) The “El Dragón Mine”, Porco, Potosí, Bolivia – Selenium minerals. *Mineral UP*, **1**, 16–25.
- Kampf A.R., Mills S.J. and Housley R.M. (2010) The crystal structure of munakataite, $\text{Pb}_2\text{Cu}_2(\text{Se}^{4+}\text{O}_3)(\text{SO}_4)(\text{OH})_4$, from Otto Mountain, San Bernardino County, California, USA. *Mineralogical Magazine*, **74**, 991–998.
- Kampf A.R., Mills S.J., Nash B.P., Thorne B. and Favreau G. (2016a) Alfredopetrovite, a new selenite mineral from the El Dragón mine, Bolivia. *European Journal of Mineralogy*, **28**, 479–484.
- Kampf A.R., Mills S.J. and Nash B.P. (2016b) Pauladamsite, $\text{Cu}_4(\text{SeO}_3)(\text{SO}_4)(\text{OH})_4 \cdot 2\text{H}_2\text{O}$, a new mineral from the Santa Rosa mine, Darwin district, California, USA. *Mineralogical Magazine*, **80**, 949–958.
- Kasatkin A.V., Plášil J., Marty J., Agakhanov A.A., Belakovskiy D.I. and Lykova I.S. (2014) Nestolaite, $\text{CaSeO}_3 \cdot \text{H}_2\text{O}$, a new mineral from the Little Eva mine, Grand County, Utah, USA. *Mineralogical Magazine*, **78**, 497–505.
- Lafuente B., Downs R.T., Yang H., Stone N. (2015) The power of databases: the RRUFF project. Pp 1–30 in: *Highlights in Mineralogical Crystallography* (T Armbruster and R M Danisi, editors). W. De Gruyter, Berlin, Germany.
- Libowitzky E. (1999) Correlation of O–H stretching frequencies and O–H...O hydrogen bond lengths in minerals. *Monatshfte für Chemie*, **130**, 1047–1059.
- Mandarino J.A. (1981) The Gladstone–Dale relationship. IV. The compatibility concept and its application. *The Canadian Mineralogist*, **19**, 441–450.
- Mills S.J., Kampf A.R., Housley R.M., Christy A.G., Thorne B., Chen Y.-S. and Steele I.M. (2014) Favreaute, a new selenite mineral from the El Dragón mine, Bolivia. *European Journal of Mineralogy*, **26**, 771–781.
- Paar W.H., Cooper M.A., Moëlo Y., Stanley C.J., Putz H., Topa D., Roberts A.C., Stirling J., Raith J.G. and Rowe R. (2012) Eldragónite, $\text{Cu}_6\text{BiSe}_4(\text{Se}_2)$, A new mineral species from the El Dragón Mine, Potosí, Bolivia and its crystal structure. *The Canadian Mineralogist*, **50**, 281–294.
- Schofield P.F., Wilson C.C., Knight K.S. and Kirk C.A. (2009) Proton location and hydrogen bonding in the hydrous lead copper sulfates linarite, $\text{PbCu}(\text{SO}_4)(\text{OH})_2$ and caledonite, $\text{Pb}_2\text{Cu}_2(\text{SO}_4)_3\text{CO}_3(\text{OH})_6$. *The Canadian Mineralogist*, **47**, 649–662.

- Sevvana M., Ruf M., Isabel Usón I., Sheldrick G.M. and Herbst-Irmere R. (2019) Non-merohedral twinning: from minerals to proteins. *Acta Crystallographica*, **D75**, 1040–1050.
- Shannon R.D. (1976) Revised effective ionic radii and systematic studies of interatomic distances in halides and chalcogenides. *Acta Crystallographica*, **A32**, 751–767.
- Sheldrick G.M. (2015a) SHELXT – Integrated space-group and crystal structure determination. *Acta Crystallographica*, **A71**, 3–8.
- Sheldrick G.M. (2015b) Crystal structure refinement with SHELX. *Acta Crystallographica*, **C71**, 3–8.
- Wickleder, M.S., Buchner, O., Wickleder, C., Sheik, S.E., Brunklaus, G. and Eckert, H. (2004) Au₂(SeO₃)₂(SeO₄): Synthesis and characterization of a new noncentrosymmetric selenite-selenate. *Inorganic Chemistry*, **43**, 5860–5864.
- Wolak J., Pawlowski A., Polomska M. and Pietraszko A. (2013) Molecular dynamics in (NH₄)₃H(SeO₄)₂ at superionic phase transitions: Raman spectroscopy study. *Phase Transitions*, **86**, 182–190.
- Yang H., McGlasson J.A., Gibbs R.B. and Downs R.T. (2022) Franksousaite, IMA 2021-096. CNMNC Newsletter 65. *Mineralogical Magazine*, **86**, 354–358.